Journal of Chemical&Engineering Data

pubs.acs.org/jced Article

Diffusion Coefficients of N_2O and H_2 in Water at Temperatures between 298.15 and 423.15 K with Pressures up to 30 MPa

Sijia Wang, Tong Zhou, Ziqing Pan, and J. P. Martin Trusler*

Cite This: *J. Chem. Eng. Data* 2023, 68, 1313−1319 Read Online

ACCESS | Metrics & More | Article Recommendations | Supporting Information

ABSTRACT: The diffusion coefficients of CO_2 and H_2 in aqueous solutions are important in numerous processes including carbon capture, geological carbon storage, and reservoir storage of hydrogen. As CO_2 is reactive in some aqueous solutions, especially aqueous amine solvents for carbon capture, N_2O is frequently studied as a surrogate. In this work, the Taylor dispersion technique was used to determine the diffusion coefficients of N_2O and H_2 at high dilution in water at temperatures between 298.15 and 423.15 K and at pressures up to 30 MPa, with a standard relative uncertainty of 1.6%. The new data are intended to resolve significant discrepancies in the literature. The results confirm that temperature is the most important controlling factor and that the diffusion coefficients are nearly independent of pressure in the region studied. The experimental data were correlated using the Stokes−Einstein equation, with average absolute relative deviations of 0.5% for both systems.

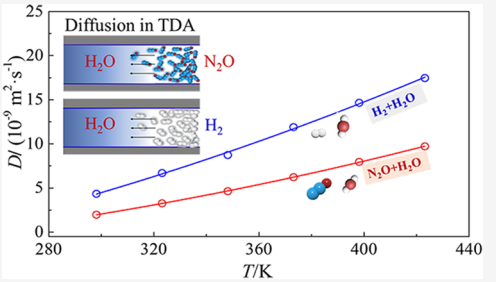

1. INTRODUCTION

The thermophysical properties of solutions of light gases in water, brine, and mixed solvent systems are important in controlling mass transfer in numerous processes, especially in the context of carbon dioxide capture, hydrogen production, and the transportation and storage of both gases.[1−3]

In carbon dioxide capture, the diffusion coefficients of CO_2 and other gases in aqueous amine solutions are an important input to the estimation of mass transfer coefficients and hence the size of process equipment.[4,5] Unfortunately, the diffusion process is complicated by rapid chemical reactions between CO_2 and the aqueous amine, making measurements of the true diffusion coefficient of molecular CO_2 in such solvents essentially impossible. Therefore, the analogy proposed by Clarke[6] is often invoked by which N_2O is taken as a surrogate for CO_2. This is motivated by the fact that the two molecules have the same mass, structure, and number of electrons but different reactivity (N_2O does not react with aqueous amines). The basic hypothesis is that the tracer diffusion coefficient $D_{CO_2}(T, p, m)$ of CO_2 in an aqueous amine solution of molality m at temperature T and pressure p may be estimated from the corresponding tracer diffusion coefficient $D_{N_2O}(T, p, m)$ of N_2O in the same amine solution and the tracer diffusion coefficients of both gases in pure H_2O as follows

$$D_{CO_2}(T, p, m) = D_{N_2O}(T, p, m)\left(\frac{D_{CO_2}(T, p, m=0)}{D_{N_2O}(T, p, m=0)}\right) \quad (1)$$

For geological carbon storage, especially in saline aquifers, the diffusion coefficients of CO_2 in brines are important factors controlling the rate of gas dissolution and long-term migration. Injected CO_2 typically contains impurities that affect mass transfer. For example, CO_2 is more soluble in aquifer brines than impurities such as N_2 and H_2[7] so that CO_2 dissolves and disperses faster, creating a zone enriched in the less-soluble impurity gases. The dissolution and mass transfer mechanisms are governed by the Henry's law constant and the diffusion coefficients are sometimes associated with subtle phenomena, such as Ostwald ripening, that can accelerate gas dissolution in the aqueous phase.[8] Similarly, modeling of processes such as hydrogen production by water electrolysis and reservoir storage of hydrogen calls for knowledge of H_2 diffusion in aqueous electrolytes. Therefore, it is important to measure the diffusion coefficients of these gases in relevant aqueous solutions over wide ranges of temperature and pressure. The systems of interest usually contain three or more components, but one should first determine the diffusivities in binary gas−water solutions.

In previous studies, the diffusion properties of gas−liquid systems were studied extensively using the laminar liquid jet absorber (LLJ), diaphragm cell (DC), wetted wall column absorber (WWA), and Taylor dispersion apparatus (TDA). These and other techniques for measuring mutual diffusion coefficients in binary systems have been reviewed in the

Received: February 8, 2023
Accepted: May 15, 2023
Published: May 25, 2023

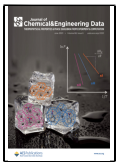

literature.[9,10] The diffusivity of CO_2 in water has been studied by several authors and may be considered as well known under conditions relevant to CO_2 capture and geological storage; the correlation of Cadogan et al. can be recommended for temperatures between (298.15 and 423.15) K.[11] Several authors have measured the diffusion coefficient of N_2O in water, and the available data are summarized in Table 1.[12−25]

Table 1. Summary of Previous Diffusion Coefficient Measurements of (N_2O + H_2O) and (H_2 + H_2O)

fluids	T/K	experimental method[a]	authors
N_2O + H_2O	293	LLJ	Thomas et al.[12]
	298−313	LLJ	Duda et al.[13]
	289.7−303.8	WWA	Davidson et al.[14]
	298	LLJ	Joosten et al.[15]
	298	LLJ	Sada et al.[16]
	288−308	LLJ	Haimour et al.[17]
	291−353	DC	Versteeg et al.[18]
	298.15	LLJ	Diaz et al.[19]
	288−323	LLJ	Al-Ghawas et al.[20]
	293−368	WWA	Tamimi et al.[21]
	303−313	WWA	Li et al.[22]
	293−313	WWA	Mandal et al.[23]
	298−313	WWA	Samanta et al.[24]
	293.15−368.15	TDA	Hamborg et al.[25]
H_2 + H_2O	283−333	CSB	Wise et al.[26]
	293−333	CSB	de Blok et al.[27]
	283−333	SLL	Verhallen et al.[28]
	283−328	TDA	Ferrell et al.[29]
	278−308	DC	Jahne et al.[30]

[a]CSB = rate of the collapse of small bubbles; LLJ = laminar liquid jet absorber; SLL = permeability of a stagnant liquid layer in the quasi-steady state; DC = diaphragm cell; WWA = wetted wall column absorber; TDA = Taylor dispersion apparatus.

Viscosity and diffusivity data have been correlated by Joosten et al.[15] and Sada et al.;[16] the diffusivity of CO_2 in aqueous solutions has also been estimated from N_2O data. CO_2 diffusivity in aqueous amine solutions was estimated by Li et al.[22] and Mandal et al.[23] using the N_2O analogy. Tamimi et al.[21] measured the aqueous-phase diffusion coefficients of H_2S, CO_2, and N_2O and compared them to experimental data and predictions based on the Wilke−Chang equation. Hamborg et al.[25] reported diffusivities of N_2O in both water and aqueous piperazine solutions and discussed some of the difficulties encountered when applying the TDA technique with a refractive index detector to three-component systems. Table 1 also summarizes the available diffusion coefficient data for the (H_2 + H_2O) system.[26−31] These five studies present data at temperatures between 278 and 333 K measured by four different experimental methods.

A comparison of the available data for both systems indicated significant disagreement between different sources; this point is discussed in Section 3. The data are also restricted to relatively low temperatures (≤368 K for N_2O and ≤333 K for H_2). Therefore, the objective of the present work was to perform new measurements of the mutual diffusion coefficient at infinite dilution of the gaseous solute for both systems using the reliable Taylor dispersion method in wide ranges of temperature and pressure. The new measurements extend in temperature from 298.15 to 423.15 K with pressures up to 30 MPa.

2. EXPERIMENTAL SECTION

2.1. Experimental Material and Apparatus. The Taylor dispersion apparatus (TDA) used has been described previously by Cadogan et al.[11] Figure 1 is a schematic diagram showing the two alternative configurations used in this work. The main components are the solvent pump, the solute injection system utilizing a six-port sample valve with 20 μL sample loop (0.5 mm ID × 100 mm long), the diffusion capillary (1.08 mm ID × 4.5 m long), and a refractive index detector (Agilent 1100 Series, RID). Pump A was an HPLC pump (Agilent 1200 Series) with a maximum operating pressure of 40 MPa, while pump B comprised a 50 mL plastic syringe mounted in a motorized syringe driver (Chemys Nexus 3000); both pumps were operated under computer control.

A vacuum degasser (Agilent 1200 Series) was used to degas the mobile phase before it entered pump A. The temperature of the capillary was controlled by a thermostatic oil bath, while the mobile-phase pressure was controlled by a combination of the back-pressure valve at the exit of the RID (V2 in Figure 1) and interchangeable restriction tubes located between the capillary and the RID (V1 in Figure 1). The restrictor tubes were of 50 μm internal diameter with lengths between 30 and 100 mm, depending upon the desired back pressure. Measurements at pressures below 1 MPa were made without a restrictor tube. The flow rate of the mobile phase was adjusted to achieve the desired pressure in the column according to the Hagen−Poiseuille equation. The temperature was measured with a platinum resistance thermometer immersed in the oil bath, and the pressure was measured

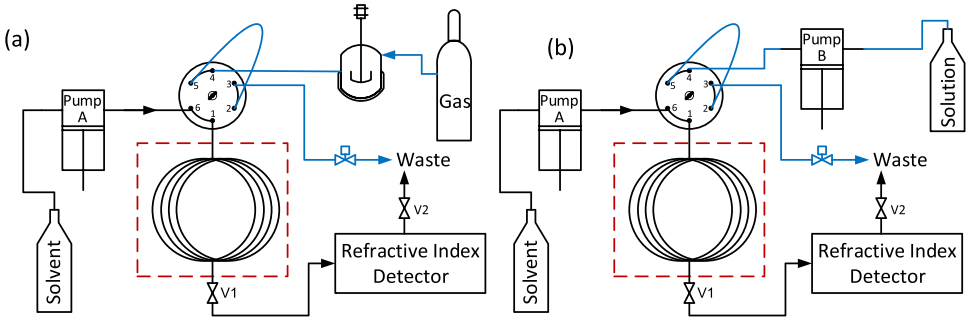

Figure 1. Schematic of the experimental system for (a) (N_2O + H_2O) and (H_2 + H_2O) fluid systems and (b) (KCl + H_2O). Pump A delivered the mobile phase (water), while pump B was for the injection of aqueous KCl. Aqueous solutions of the gases were injected from the pressure vessel shown in (a). V1 is the post column restrictor tube, and V2 is the post detector back-pressure valve.

https://doi.org/10.1021/acs.jced.3c00085
J. Chem. Eng. Data 2023, 68, 1313−1319

Table 2. Description of Chemical Samples, Where x is the Mole Fraction, w is the Mass Fraction, and ρ_e is the Electrical Resistivity

chemical name	CAS number	source	purity as supplied[a]	additional purification
nitrous oxide	10024-97-2	BOC	$x \geq 0.99995$	none
hydrogen	1333-74-0	BOC	$x \geq 0.99995$	none
potassium chloride	7447-40-7	Sigma-Aldrich	$w \geq 0.99$	none
water	7732-18-5	Millipore	$\rho_e \geq 18$ MΩ at 298 K	vacuum degassing

[a]Purities are as stated by the supplier.

upstream of the capillary using the strain−gauge pressure sensor integrated in the solvent pump. The RID was operated at a constant temperature of 308.15 K and incorporated an internal heat exchanger to bring the flow to that temperature prior to entering the refractive index cell.

The two alternative configurations shown in Figure 1 differ in respect of the method by which the sample is introduced. In configuration (a), a quantity of the mobile phase was loaded into a 100 mL stirred vessel and presaturated with a gaseous solute at a pressure of approximately 0.7 MPa. The saturated solution was then used to fill the sample loop prior to injection, a back-pressure valve located in the exit stream preventing degassing during the filling of the loop. In configuration (b), a solution of a nonvolatile solute was loaded into a syringe pump from which the sample loop was then filled.

The details of the chemical samples used in this work can be found in Table 2. Pure deionized water was used as the mobile phase. Aqueous potassium chloride solution of molality 0.1 mol·kg^{-1} was injected for validation measurements. The N_2O and H_2 were the gaseous solutes studied.

2.2. Measurement Procedure. Before each measurement campaign, the system was flushed extensively with DI water. The RID purge valve and the six-port sample valve were alternately switched during this procedure. The flow rate of the mobile phase was adjusted to achieve approximately the desired pressure in the diffusion capillary. For measurements on gaseous solutes, approx. 80 mL of the mobile phase was added to the saturation vessel together with a magnetic stirrer bar. This sample was degassed under vacuum with stirring for approx. 30 min before being saturated with the gas under study at a pressure of between (0.5 and 0.7) MPa. After a few minutes to allow for sufficient dissolution of the gas, the magnetic stirrer was turned off. For the validation measurements, aqueous KCl solution (0.1 mol·kg^{-1}) was prepared, degassed under vacuum, and loaded into syringe pump B (Figure 1b). Injection of a sample was accomplished by first flushing the sample loop with solution and then switching the six-port valve to the inject position for approx. 5 s. Depending upon the flow rate of the mobile phase, elution times were in the range of 700−1100 s.

The RID signal $s(t)$ was recorded and subsequently analyzed to obtain the diffusion coefficient D according to the theory of Aris,[32] incorporating small corrections as detailed in the Supporting Information. These corrections account for the interconnecting tubing on either side of the diffusion column, including the restrictor tubes, as detailed previously by Cadogan et al.[11] and for the finite volume of the injection loop. These corrections are incorporated in the model as contributions to the effective length of the diffusion column. The combined corrections amount to less than 2% of the column length at the lowest temperature studied, increasing to nearly 10% of the column length at the highest temperature studied. The analysis of the RID signal made allowance for baseline drift as a linear function of time. Such drift was always a small fraction of the peak signal over the period of solute elution. Measurements were repeated at least five times. In all cases, the quantity measured is the mutual diffusion coefficient at effectively infinite dilution of the solute; for simplicity, we denote this simply as D. In order to minimize error due to secondary flow in the coiled diffusion column, the dimensionless group De^2Sc should be minimized.[25] The effect of finite De^2Sc is discussed by Cadogan et al.,[11] who show that the relative error is approximately $(De^2Sc/653)$.[2] In this study, De^2Sc was <43 for (N_2O + H_2O) and <19 for (H_2 + H_2O), leading to small relative corrections of <0.4% and <0.1%, respectively. Figure 2a shows a typical sequence of chromatographic peaks corresponding to five injections for the N_2O−water system at T = 423 K and p = 5.6 MPa. Figure 2b is an enlargement of the third peak showing the experimental refractive index data (collected at 5 s time intervals) with the Aris model[32] incorporating corrections as detailed in the

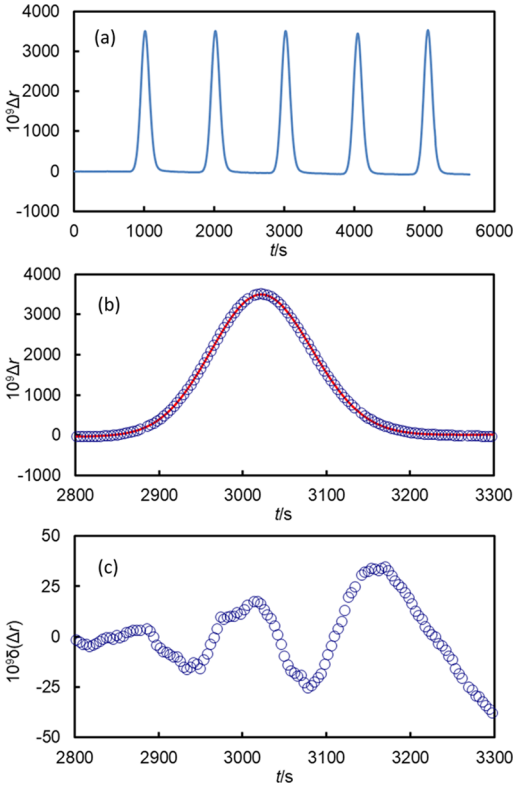

Figure 2. (a) Differential refractive index Δr as a function of time t for five injection of N_2O(aq) into water at T = 423 K and p = 5.6 MPa. (b) Enlargement of the third peak comparing experimental data (○) with the fitted model (—). (c) Deviations $\delta(\Delta r)$ of the differential refractive index from the fitted model for the analysis of the third peak.

https://doi.org/10.1021/acs.jced.3c00085
J. Chem. Eng. Data 2023, 68, 1313−1319

Supporting Information. Finally, Figure 2c shows the deviations of the refractive index data from the fitted model; in relative terms, these deviations fall within about ±1% of the peak signal.

The pressure and temperature of the saturator vessel were such that, when the solution was injected into the mobile phase, the flow remained single phase. During the passage through the column, the concentration of solute rapidly declines as a result of the axial dispersion, and this ensures that the gas remains in solution even when the pressure is reduced at the detector.

2.3. Uncertainty Analysis. The combined standard relative uncertainties associated with the diffusion coefficients were calculated from the relation

$$u_r^2(D) = u_r^2(K) + 4u_r^2(R) + 4u_r^2(v) + [p(\partial \ln D/\partial p)_T u_r(p)]^2 + [(\partial \ln D/\partial T)_p u(T)]^2 \quad (2)$$

Here, $u_r(X)$ and $u(X)$ denote standard relative uncertainty and standard uncertainty of quantity X, respectively; K is the dispersion coefficient; R is the column radius; v is the superficial flow velocity; p is pressure; and T is temperature. The standard relative uncertainty of the dispersion coefficient was taken as the standard deviation of a typical set of repeated measurements from which K was determined, which is 1.5%, while $u_r(R) = 0.22\%$,[33] $u_r(v) = 0.35\%$, $u_r(p) = 0.25\%$, and $u(T) = 0.15$ K. Combining all terms, the expanded relative uncertainty of D was 3.2% with a coverage factor $k = 2$.

3. RESULTS AND DISCUSSION

3.1. Validation. The apparatus used in the present study has been used previously to measure the mutual diffusion coefficients of KCl,[33] CO_2, and N_2 in water[11] and of CO_2 and CH_4 in various hydrocarbons.[34−36] An additional validation experiment was conducted by measuring the diffusion coefficient of KCl in water at a pressure of 0.6 MPa. The results were 1.89×10^{-9} m^2·s^{-1} at $T = 298.15$ K, and 4.44×10^{-9} m^2·s^{-1} at $T = 348.15$ K. The results are shown in Figure 3 together with data from the literature, and one can observe generally good agreement. The present data are fractionally lower than those reported by Secuianu et al.[33] by 2.8% at $T = 298.15$ K and 0.9% at $T = 348.15$ K.

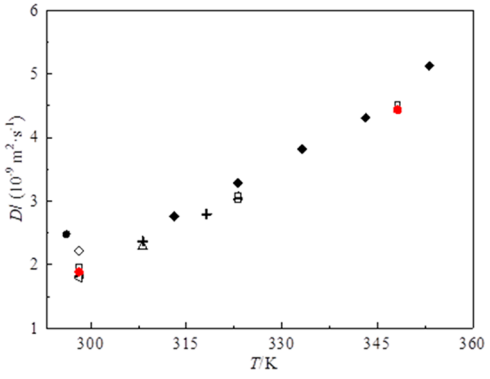

Figure 3. Comparison of the diffusion coefficient D of KCl in water: ◊, Tanaka et al.;[37] +, Firth et al.;[38] ■, Rard et al.;[39] ◁, Leaist et al.;[40] ●, McCall et al.;[41] ▲, Yeh et al.;[42] ▼, Collings et al.;[43] ◆, Fell et al.;[44] □, Secuianu et al.;[33] △, Vitagliano et al.;[45] red solid circle, this work.

3.2. Diffusion Coefficients of N_2O in Water. N_2O diffusivities at infinite dilution in pure water were measured at 25 K intervals over the temperature range (298−423) K and in the pressure range (0.6−25.3) MPa. The results are reported in Table 3. As expected, the pressure proved to have only a marginal effect on the measured values of the diffusion coefficient. Figure 4 shows the present results plotted as a function of temperature in comparison with data from the literature, most of which were measured at or near ambient pressure. Compared with the literature, one can observe quite large discrepancies. For instance, Tamimi et al.[21] used a wetted-sphere apparatus to measure D at temperatures from 293.15 to 368.15 K and their results are 42% higher on average than the current data. Hamborg et al.[25] used the same method (TDA) as in the current study to measure D at temperatures

Table 3. Diffusion Coefficients D and Standard Deviations σ_D/D for N_2O in Water at Temperatures T and Pressure p Determined from N Repeated Injections.[a]

T/K	p/MPa	$D/(10^{-9}$ m^2·s$^{-1})$	N	$10^2(\sigma_D/D)$
298.15	0.6	1.971	8	0.7
323.15	0.6	3.319	6	1.0
348.15	5.6	4.793	5	0.6
373.15	5.7	6.524	5	0.6
398.15	5.7	8.578	5	0.5
423.15	5.7	10.68	7	1.3
298.15	24.7	1.912	8	0.6
323.15	24.8	3.217	6	0.5
348.15	25.0	4.801	7	0.5
373.15	25.1	6.675	6	0.4
398.15	25.3	8.704	5	1.3
423.15	25.1	10.96	5	0.3

[a]Standard uncertainties are $u(T) = 0.15$ K, $u(p) = 0.1$ MPa, and $u(D) = 0.016D$.

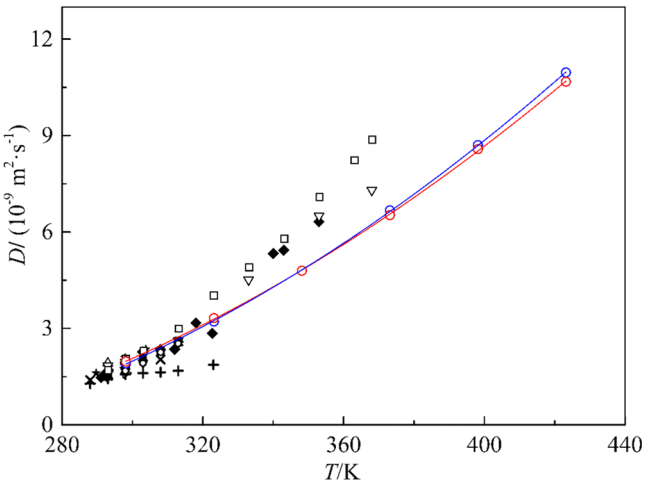

Figure 4. Comparison of the diffusion coefficient D of N_2O in water with previous data: △, Thomas et al.;[12] ▲, Duda et al.;[13] ★, Davidson et al.;[14] ◊, Joosten et al.;[15] ◀, Sada et al.;[16] ×, Haimour et al.;[17] ◆, Versteeg et al.;[18] ▷, Diaz et al.;[19] +, Al-Ghawas et al.;[20] ▽, Tamimi et al.;[21] ■, Li et al.;[22] ●, Mandal et al.;[23] ○, Samanta et al.;[24] □, Hamborg et al.;[25] blue circle, this work in the pressure range (0.6 to 5.7) MPa; blue line, Stokes−Einstein correlation at $p = 1$ MPa; red circle, this work in the pressure range (24.7 to 25.3) MPa; red line, Stokes−Einstein correlation at $p = 25$ MPa.

https://doi.org/10.1021/acs.jced.3c00085
J. Chem. Eng. Data 2023, 68, 1313−1319

from 293.15 to 368.15 K. These data are in near agreement with the present results at low temperatures but, surprisingly, they show rapidly increasing deviations with increasing temperature. On the other hand, some measurements made using laminar liquid jet absorbers are significantly lower than this work.[17,20]

The new data were correlated in terms of the modified Stokes−Einstein equation

$$D = k_B T/(n_{SE}\pi\eta a) \quad (3)$$

Here, k_B is the Boltzmann constant, n_{SE} is the Stokes−Einstein number, η is the solvent viscosity, and a is the hydrodynamic radius of the solute, which was represented as a weak function of temperature and pressure by the relation

$$a = a_0[1 + a_{10}\theta + a_{01}\varphi + a_{11}\theta\varphi] \quad (4)$$

where $\theta = T/\mathrm{K} - 298.15$ and $\varphi = p/\mathrm{MPa}$. In this work, n_{SE} was taken to be 4, corresponding to the theoretical result for a spherical particle with a slip boundary condition.[46] The viscosity of water was calculated from the IAPWS recommended correlation.[47] The parameters a_0, a_{10}, a_{01}, and a_{11} were adjusted to best fit the present data and are given in Table 4.

Table 4. Parameters a_0, a_{10}, a_{01}, and a_{11} in Eq 4 for the Hydrodynamic Radii of N_2O and H_2 in Aqueous Solution

solute	a_0/pm	a_{10}	a_{01}	a_{11}
N_2O	186.75	2.39×10^{-3}	1.56×10^{-3}	-4.14×10^{-5}
H_2	86.47	5.42×10^{-3}	-3.43×10^{-4}	-4.25×10^{-5}

Figure 4 shows the Stokes−Einstein correlation evaluated at pressures of 1 and 25 MPa and illustrates the good representation of the new data that this simple model provides. This is illustrated further in Figure 5, which shows the relative deviations between the present results and the Stokes−Einstein model. The average absolute relative deviation is 0.5%.

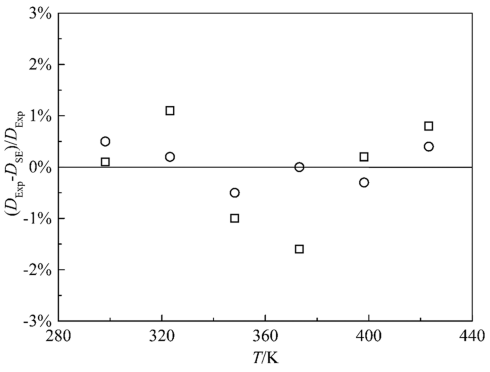

Figure 5. Deviations of experimental diffusion coefficients D_{Exp} from the values D_{SE} calculated from the modified Stokes−Einstein correlation for N_2O in water: □, data for the pressure range (0.6 to 5.7) MPa; ○, data for the pressure range (24.7 to 25.3) MPa.

3.3. Diffusion Coefficients of H_2 in Water. The diffusivities of H_2 at infinite dilution in water were also measured at temperatures ranging from 298 to 423 K and at a pressure of 0.4−30.2 MPa. The results, reported in Table 5, are compared with data from the literature in Figure 6. Again, there are quite large discrepancies with and between different literature sources. In particular, the measurements of Wise et al.[26] by the rate of bubble-collapse method show increasing positive deviation with increasing temperature.

Table 5. Diffusion Coefficients D and Standard Deviations σ_D/D for H_2 in Water at Temperatures T and Pressure p Determined from N Repeated Injections[a]

T/K	p/MPa	$D/(10^{-9}$ m^2·s$^{-1})$	N	$10^2(\sigma_D/D)$
298.15	0.5	4.270	9	0.6
323.15	0.5	6.613	6	1.0
348.15	0.4	9.210	4	0.9
373.15	0.5	11.94	5	2.3
398.15	0.4	14.83	10	1.6
298.15	27.9	4.333	10	1.2
323.15	28.7	6.806	5	1.2
373.15	28.0	12.37	5	0.5
398.15	27.9	15.55	6	0.5
423.15	28.3	18.86	9	0.6

[a]Standard uncertainties are $u(T) = 0.15$ K, $u(p) = 0.1$ MPa, and $u(D) = 0.016D$.

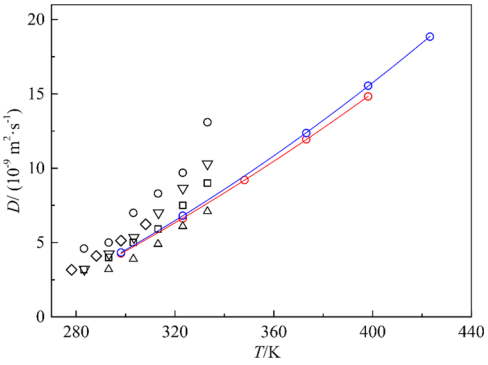

Figure 6. Comparison of the diffusion coefficient D of H_2 in water with previous data: △, de Blok et al.;[27] ○, Wise et al.;[26] □, Ferrell et al.;[29] ◊, Jahne et al.;[30] ▽, Verhallen et al.;[28] blue circle, this work in the pressure range (0.4 to −0.5) MPa; blue line, Stokes−Einstein correlation at $p = 0.5$ MPa; red circle, this work in the pressure range (27.9 to 28.7) MPa; red line, Stokes−Einstein correlation at $p = 28$ MPa.

The present data were correlated by the modified Stokes−Einstein model with hydrodynamic radius according to eq 4 with the parameters given in Table 4. In this case, the average absolute relative deviation is also 0.5%. Curves according to the model at pressures of 1 and 25 MPa are plotted in Figure 5, and deviations of the measured values from the model are shown in Figure 7.

4. DISCUSSION AND CONCLUSIONS

The Taylor dispersion method was used in this study to determine the mutual diffusion coefficient for N_2O and H_2 in water at effectively infinite dilution between 298 and 423 K with pressures up to 30 MPa, with expanded relative uncertainties of about 3.2%. The results could be correlated with the Stokes−Einstein equation incorporating a weakly temperature- and pressure-dependent hydrodynamic radius, with absolute relative deviations of 0.5%. The diffusion coefficients of N_2O and H_2 in water are nearly pressure-independent, which is consistent with the low compressibility of the solvent, although the effect of pressure is more noticeable as the temperature increases. The differences between the diffusion coefficients of N_2O and H_2 in water are driven by the effective size of the solutes, both of which are

https://doi.org/10.1021/acs.jced.3c00085
J. Chem. Eng. Data 2023, 68, 1313−1319

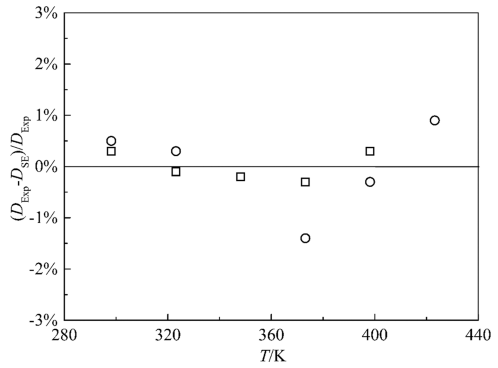

Figure 7. Deviations of experimental diffusion coefficients D_{Exp} from the values D_{SE} calculated from the modified Stokes−Einstein equation for H_2 in water: □, data for the pressure range (0.4 to 0.5) MPa; ○, data for the pressure range (27.9 to 28.7) MPa.

linear molecules. The hydrodynamic radii obtained at T = 298.15 K and p = 0.1 MPa are approx. 187 pm for N_2O and 86 pm H_2.

Previous studies of the diffusion coefficient of N_2O and H_2 in water show poor agreement, especially at elevated temperatures. The present work is intended to resolve these discrepancies by providing data over an extended range of temperatures measured by a well-established and validated experimental technique. The results are of value in at least two specific contexts: the use of N_2O as a nonreactive surrogate for CO_2 in aqueous solutions and modeling of underground hydrogen storage in water-wet porous reservoir rocks.

■ ASSOCIATED CONTENT

Supporting Information

The Supporting Information is available free of charge at https://pubs.acs.org/doi/10.1021/acs.jced.3c00085.

Details for the working equation for the Taylor dispersion apparatus incorporating corrections (PDF)

■ AUTHOR INFORMATION

Corresponding Author

J. P. Martin Trusler − *Department of Chemical Engineering, Imperial College London, London SW7 2AZ, U.K.;* orcid.org/0000-0002-6403-2488; Email: m.trusler@imperial.ac.uk

Authors

Sijia Wang − *Department of Chemical Engineering, Imperial College London, London SW7 2AZ, U.K.; Key Laboratory of Ocean Energy Utilization and Energy Conservation of the Ministry of Education, Dalian University of Technology, Dalian 116024, P. R. China*

Tong Zhou − *Department of Chemical Engineering, Imperial College London, London SW7 2AZ, U.K.*

Ziqing Pan − *Department of Chemical Engineering, Imperial College London, London SW7 2AZ, U.K.; Institute of Energy, Peking University, Beijing 100871, P. R. China*

Complete contact information is available at: https://pubs.acs.org/10.1021/acs.jced.3c00085

Notes

The authors declare no competing financial interest.

■ ACKNOWLEDGMENTS

This work was supported in part by a scholarship awarded by the China Scholarship Council.

■ REFERENCES

(1) Hassanpouryouzband, A.; Joonaki, E.; Edlmann, K.; Heinemann, N.; Yang, J. Thermodynamic and transport properties of hydrogen containing streams. *Sci. Data* **2020**, *7*, No. 222.

(2) Lozano-Martín, D.; Moreau, A.; Chamorro, C. R. Thermophysical properties of hydrogen mixtures relevant for the development of the hydrogen economy: Review of available experimental data and thermodynamic models. *Renewable Energy* **2022**, *198*, 1398−1429.

(3) Trusler, J. P. M. Thermophysical properties and phase behavior of fluids for application in carbon capture and storage processes. *Annu. Rev. Chem. Biomol. Eng.* **2017**, *8*, 381−402.

(4) Lu, W.; Guo, H.; Chou, I. M.; Burruss, R. C.; Li, L. Determination of diffusion coefficients of carbon dioxide in water between 268 and 473 K in a high-pressure capillary optical cell with in situ raman spectroscopic measurements. *Geochim. Cosmochim. Acta* **2013**, *115*, 183−204.

(5) Ünveren, E. E.; Monkul, B. Ö.; Sarıoğlan, Ş.; Karademir, N.; Alper, E. Solid amine sorbents for CO_2 capture by chemical adsorption: A review. *Petroleum* **2017**, *3*, 37−50.

(6) Clarke, J. K. A. Kinetics of absorption of cardon dioxide in monoethanolamine solutions at short contact times. *Ind. Eng. Chem. Fundam.* **1964**, *3*, 239−245.

(7) Hashemi, L.; Blunt, M.; Hajibeygi, H. Pore-scale modelling and sensitivity analyses of hydrogen-brine multiphase flow in geological porous media. *Sci. Rep.* **2021**, *11*, No. 8348.

(8) Blunt, M. J. Ostwald ripening and gravitational equilibrium: Implications for long-term subsurface gas storage. *Phys. Rev. E* **2022**, *106*, No. 045103.

(9) Wakeham, W. A.; Nagashima, A.; Sengers, J. V. Measurement of the Transport Properties of Fluids. In *Experimental Thermodynamics*; Blackwell: Oxford, 1991; Vol. *III*.

(10) Assael, M. J.; Vesovic, V.; Wakeham, W. A.Advances in Transport Properties of Fluids. In *Experimental Thermodynamics*; Royal society of Chemistry, 2014; Vol. *IX*, p 401.

(11) Cadogan, S. P.; Maitland, G. C.; Trusler, J. P. M. Diffusion coefficients of CO_2 and N_2 in water at temperatures between 298.15 K and 423.15 K at pressures up to 45 MPa. *J. Chem. Eng. Data* **2014**, *59*, 519−525.

(12) Thomas, W. J.; Adams, M. J. Measurement of the diffusion coefficients of carbon dioxide and nitrous oxide in water and aqueous solutions of glycerol. *Trans. Faraday Soc.* **1965**, *61*, 668−673.

(13) Duda, J. L.; Vrentas, J. S. Laminar liquid jet diffusion studies. *AIChE J.* **1968**, *14*, 286−294.

(14) Davidson, J. The determination of diffusion coefficient for sparingly soluble gases in liquids. *Trans. Inst. Chem. Eng.* **1957**, *35*, 51−60.

(15) Joosten, G. E. H.; Danckwerts, P. V. Solubility and diffusivity of nitrous oxide in equimolar potassium carbonate-potassium bicarbonate solutions at 25° and 1 atm. *J. Chem. Eng. Data* **1972**, *17*, 452−454.

(16) Sada, E.; Kumazawa, H.; Butt, M. A. Solubility and diffusivity of gases in aqueous solutions of amines. *J. Chem. Eng. Data* **1978**, *23*, 161−163.

(17) Haimour, N.; Sandall, O. C. Absorption of carbon-dioxide into aqueous methyldiethanolamine. *Chem. Eng. Sci.* **1984**, *39*, 1791−1796.

(18) Versteeg, G. F.; van Swaaij, W. P. M. On the kinetics between CO_2 and alkanolamines both in aqueous and non-aqueous solutions—1. Primary and secondary amines. *Chem. Eng. Sci.* **1988**, *43*, 573−585.

(19) Diaz, J. M.; Vega, A.; Coca, J. Diffusivities of carbon dioxide and nitrous oxide in aqueous alcohol solutions. *J. Chem. Eng. Data* **1988**, *33*, 10−12.

(20) Al-Ghawas, H. A.; Hagewiesche, D. P.; Ruiz-Ibanez, G.; Sandall, O. C. Physicochemical properties important for carbon dioxide

absorption in aqueous methyldiethanolamine. *J. Chem. Eng. Data* **1989**, *34*, 385−391.
(21) Tamimi, A.; Rinker, E. B.; Sandall, O. C. Diffusion coefficients for hydrogen sulfide, carbon dioxide, and nitrous oxide in water over the temperature range 293-368 K. *J. Chem. Eng. Data* **1994**, *39*, 330−332.
(22) Li, M.-H.; Lai, M.-D. Solubility and diffusivity of N_2O and CO_2 in (monoethanolamine + n-methyldiethanolamine + water) and in (monoethanolamine + 2-amino-2-methyl-1-propanol + water). *J. Chem. Eng. Data* **1995**, *40*, 486−492.
(23) Mandal, B. P.; Kundu, M.; Padhiyar, N. U.; Bandyopadhyay, S. S. Physical solubility and diffusivity of N_2O and CO_2 into aqueous solutions of (2-amino-2-methyl-1-propanol + diethanolamine) and (n-methyldiethanolamine + diethanolamine). *J. Chem. Eng. Data* **2004**, *49*, 264−270.
(24) Samanta, A.; Roy, S.; Bandyopadhyay, S. S. Physical solubility and diffusivity of N_2O and CO_2 in aqueous solutions of piperazine and (n-methyldiethanolamine + piperazine). *J. Chem. Eng. Data* **2007**, *52*, 1381−1385.
(25) Hamborg, E. S.; Derks, P. W. J.; Kersten, S. R. A.; Niederer, J. P. M.; Versteeg, G. F. Diffusion coefficients of N_2O in aqueous piperazine solutions using the taylor dispersion technique from (293 to 333) K and (0.3 to 1.4) mol·dm^{-3}. *J. Chem. Eng. Data* **2008**, *53*, 1462−1466.
(26) Wise, D. L.; Houghton, G. The diffusion coefficients of ten slightly soluble gases in water at 10-60 °C. *Chem. Eng. Sci.* **1966**, *21*, 999−1010.
(27) de Blok, W. J.; Fortuin, J. M. H. Method for determining diffusion coefficients of slightly soluble gases in liquids. *Chem. Eng. Sci.* **1981**, *36*, 1687−1694.
(28) Verhallen, P. T. H. M.; Oomen, L. J. P.; Elsen, A. J. J. M. v. d.; Kruger, J.; Fortuin, J. M. H. The diffusion coefficients of helium, hydrogen, oxygen and nitrogen in water determined from the permeability of a stagnant liquid layer in the quasi-s. *Chem. Eng. Sci.* **1984**, *39*, 1535−1541.
(29) Ferrell, R. T.; Himmelblau, D. M. Diffusion coefficients of hydrogen and helium in water. *AIChE J.* **1967**, *13*, 702−708.
(30) Jähne, B.; Heinz, G.; Dietrich, W. Measurement of the diffusion coefficients of sparingly soluble gases in water. *J. Geophys. Res.* **1987**, *92*, 10767−10776.
(31) Ferrell, R. T.; Himmelblau, D. M. Diffusion coefficients of nitrogen and oxygen in water. *J. Chem. Eng. Data* **1967**, *12*, 111−115.
(32) Aris, R. On the dispersion of a solute in a fluid flowing through a tube. *Proc. R. Soc. London, Ser. A* **1956**, *235*, 67−77.
(33) Secuianu, C.; Maitland, G. C.; Trusler, J. P. M.; Wakeham, W. A. Mutual diffusion coefficients of aqueous KCl at high pressures measured by the taylor dispersion method. *J. Chem. Eng. Data* **2011**, *56*, 4840−4848.
(34) Cadogan, S. P.; Mistry, B.; Wong, Y.; Maitland, G. C.; Trusler, J. P. M. Diffusion coefficients of carbon dioxide in eight hydrocarbon liquids at temperatures between (298.15 and 423.15) K at pressures up to 69 MPa. *J. Chem. Eng. Data* **2016**, *61*, 3922−3932.
(35) Taib, M. B. M.; Trusler, J. P. M. Diffusion coefficients of methane in methylbenzene and heptane at temperatures between 323 K and 398 K at pressures up to 65 MPa. *Int. J. Thermophys.* **2020**, *41*, No. 119.
(36) Taib, M. B. M.; Trusler, J. P. M. Correction to: Diffusion coefficients of methane in methylbenzene and heptane at temperatures between 323 K and 398 K at pressures up to 65 MPa. *Int. J. Thermophys.* **2020**, *41*, No. 154.
(37) Tanaka, K. Effect of electrolytes on the self-diffusion coefficient of water. *J. Chem. Soc., Faraday Trans. 1* **1976**, *72*, 1121−1123.
(38) Firth, J. G.; Tyrrell, H. J. V. Diffusion coefficients for aqueous silver nitrate solutions at 25°, 35°, and 45° from diaphragm-cell measurements. *J. Chem. Soc.* **1962**, *381*, 2042−2047.
(39) Rard, J. A.; Miller, D. G. Mutual diffusion coefficients of barium chloride-water and potassium chloride-water at 25 °C from Rayleigh interferometry. *J. Chem. Eng. Data* **1980**, *25*, 211−215.
(40) Leaist, D. G.; Hao, L. Gravitational stability of taylor dispersion profiles. Revised diffusion coefficients for barium chloride-potassium chloride-water. *J. Phys. Chem. A* **1993**, *97*, 1464−1469.
(41) McCall, D. W.; Douglass, D. C. The effect of ions on the self-diffusion of water. I. Concentration dependence. *J. Phys. Chem. A* **1965**, *69*, 2001−2011.
(42) Yeh, H. S.; Wills, G. B. Diffusion coefficient of sodium nitrate in aqueous solution at 25 °C as a function of concentration from 0.1 to 1.0m. *J. Chem. Eng. Data* **1970**, *15*, 187−189.
(43) Collings, A. F.; Hall, D. C.; Mills, R.; Woolf, L. A. A conductance-monitored diaphragm cell for diffusion measurements. *J. Phys. E* **1971**, *4*, No. 425.
(44) Fell, C. J. D.; Hutchison, H. P. Diffusion coefficients for sodium and potassium chlorides in water at elevated temperatures. *J. Chem. Eng. Data* **1971**, *16*, 427−429.
(45) Vitagliano, V.; Lyons, P. A. Diffusion coefficients for aqueous solutions of sodium chloride and barium chloride. *J. Am. Chem. Soc.* **1956**, *78*, 1549−1552.
(46) Himmelblau, D. M. Diffusion of dissolved gases in liquids. *Chem. Rev.* **1964**, *64*, 527−550.
(47) Huber, M. L.; Perkins, R. A.; Laesecke, A.; Friend, D. G.; Sengers, J. V.; Assael, M. J.; Metaxa, I. N.; Vogel, E.; Mares, R.; Miyagawa, K. New international formulation for the viscosity of H_2O. *J. Phys. Chem. Ref. Data* **2009**, *38*, 101−125.

https://doi.org/10.1021/acs.jced.3c00085
J. Chem. Eng. Data 2023, 68, 1313−1319